Supplementary materials

A Minimalist and Robust Chemo-Photothermal Nanoplatform Capable of Augmenting Autophagy-Modulated Immune Response Against Breast Cancer

Hui Ming [a,1], Bowen Li [a,1], Hailong Tian [a,1], Li Zhou [a], Jingwen Jiang [a], Tingting Zhang [a], Ling Qiao [b], Peijie Wu [b], Edouard C. Nice [c], Wei Zhang [d,e], Weifeng He [f,#], Canhua Huang [a,#], and Haiyuan Zhang [g,#].

[a] *State Key Laboratory of Biotherapy and Cancer Center, West China Hospital and West China School of Basic Medical Sciences and Forensic Medicine, Sichuan University and Collaborative Innovation Center for Biotherapy, Chengdu, 610041, P.R. China.*

[b] *School of Basic Medical Sciences, Chengdu University of Traditional Chinese Medicine, Chengdu, China.*

[c] *Department of Biochemistry and Molecular Biology, Monash University, Clayton, VIC 3800, Australia.*

[d] *West China Biomedical Big Data Center, West China Hospital, Sichuan University, Chengdu 610041, China.*

[e] *Mental Health Center and Psychiatric Laboratory, the State Key Laboratory of Biotherapy, West China Hospital of Sichuan University, Chengdu, China.*

[f] *Institute of Burn Research, Southwest Hospital, State Key Laboratory of Trauma, Burn and Combined Injury, Chongqing Key Laboratory for Disease Proteomics, Army Military Medical University, Chongqing 400038, China.*

[g] *School of Basic Medicine, Health Science Center, Yangtze University, Jingzhou, China.*

[1] *These authors contributed equally to this work.*

[#] *Corresponding authors*

Email Addresses: hyzhang_88@163.com (H. Zhang); hcanhua@scu.edu.cn (C. Huang); whe761211@hotmail.com (W. He).

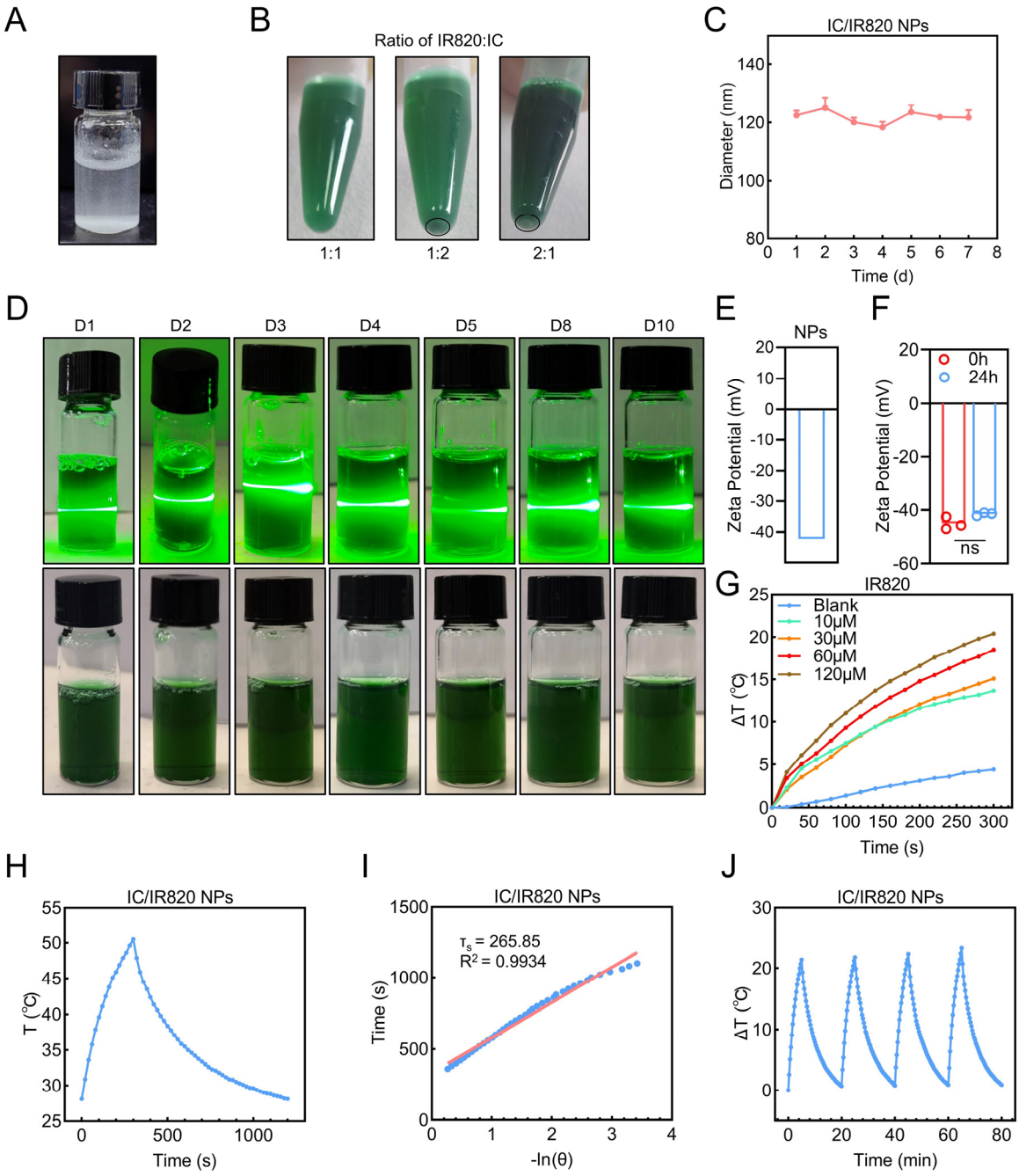

Figure S1. Preparation and stability of IC/IR820 NPs. (A) Solubility of itraconazole in water. (B) Stability of IC/IR820 NPs with different ratios. (C) Diameter of IC/IR820 nanoparticles at indicated time points. (D) Photographs of IC/IR820 NPs at indicated time points. (E) Zeta potential of IC/IR820 NPs. (F) Comparison of the Zeta potential of IC/IR820 NPs at 0 h and 24 h. (G) Photothermal activity of IR820 dispersed in water at various concentrations (λ = 808 nm, P = 1.0

W/cm^2; the irradiation time = 5 min). (H) Temperature profile of IC/IR820 NPs in water after 300 s irradiation (λ = 808 nm, P=1.0 W/cm^2) (I) Linear time data versus -ln(θ) obtained from the cooling period of IC/IR820 NPs. (J) Photothermal stability characterization using 808 nm laser irradiation (1 W/cm^2) of the IC/IR820 NPs for four heating-cooling cycles.

Calculation of the photothermal conversion efficiency

The photothermal conversion efficiency (η) of IC/IR820 nanoparticles was calculated according the following method.

$$\eta(\%)=\frac{hS\Delta T_{max}-Q_{Dis}}{I(1-10^{-A_\lambda})}\times 100\%$$

In detail,

$$hS=\frac{mC}{\tau_s}$$

$$\tau_s=-\frac{t}{\ln(\theta)}$$

$$\theta=\frac{T-T_{surr}}{\Delta T_{max}}$$

Q_{Dis} was measured to be mW using water without IC/IR820 nanoparticles. m is the mass of the solution (1.0 g), C is the heat capacity of the water solution (4.2 J/g). τ_s is the associated time constant, which was showed in Figure S1J-K.

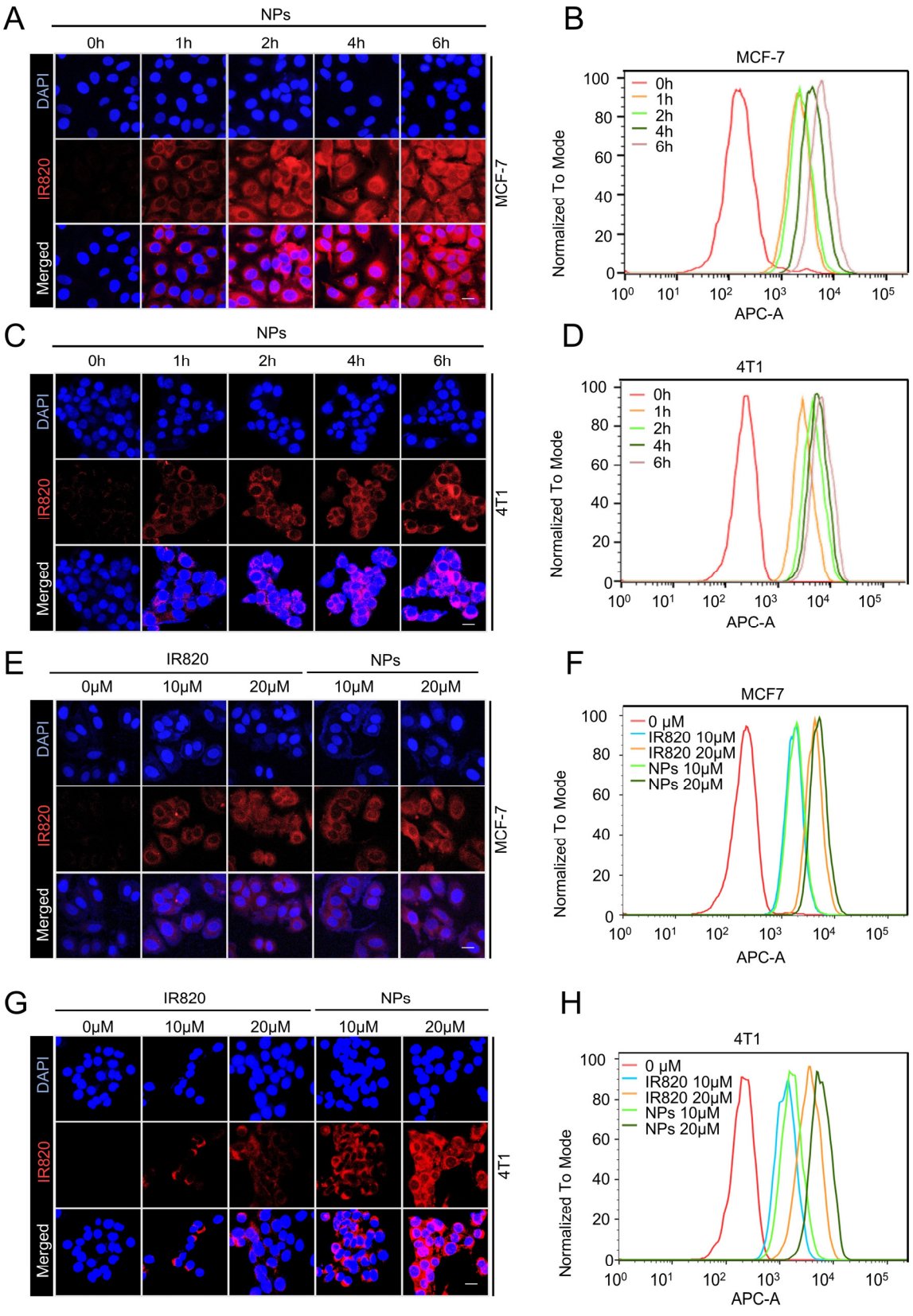
A
NPs
0h
1h
2h
4h
6h
DAPI
IR820
Merged
MCF-7
B
MCF-7
0h
1h
2h
4h
6h
Normalized To Mode
APC-A
C
NPs
0h
1h
2h
4h
6h
DAPI
IR820
Merged
4T1
D
4T1
0h
1h
2h
4h
6h
Normalized To Mode
APC-A
E
IR820
NPs
0μM
10μM
20μM
10μM
20μM
DAPI
IR820
Merged
MCF-7
F
MCF7
0 μM
IR820 10μM
IR820 20μM
NPs 10μM
NPs 20μM
Normalized To Mode
APC-A
G
IR820
NPs
0μM
10μM
20μM
10μM
20μM
DAPI
IR820
Merged
4T1
H
4T1
0 μM
IR820 10μM
IR820 20μM
NPs 10μM
NPs 20μM
Normalized To Mode
APC-A

Figure S2. Intracellular uptake of IC/IR820 NPs in MCF-7 and 4T1 cell line. (A-D) Fluorescence microscopy images and flow cytometric results show the uptake of IC/IR820 nanoparticles on indicated time points in MCF-7 and 4T1 cells. Scale bar: 20 μm. (E-H) Fluorescence microscopy images and flow cytometric results show the uptake of free IR820 and IC/IR820 nanoparticles with different concentrations in MCF-7 and 4T1 cells. Scale bar: 20 μm.

A

IC50 of IC/IR820 NPs + L (μM)

Cell line	Equivalent to IR820 (μM)	Equivalent to IC (μM)
MDA-MB-231	11.60	13.92
MCF-7	5.088	6.105
4T1	5.021	6.026

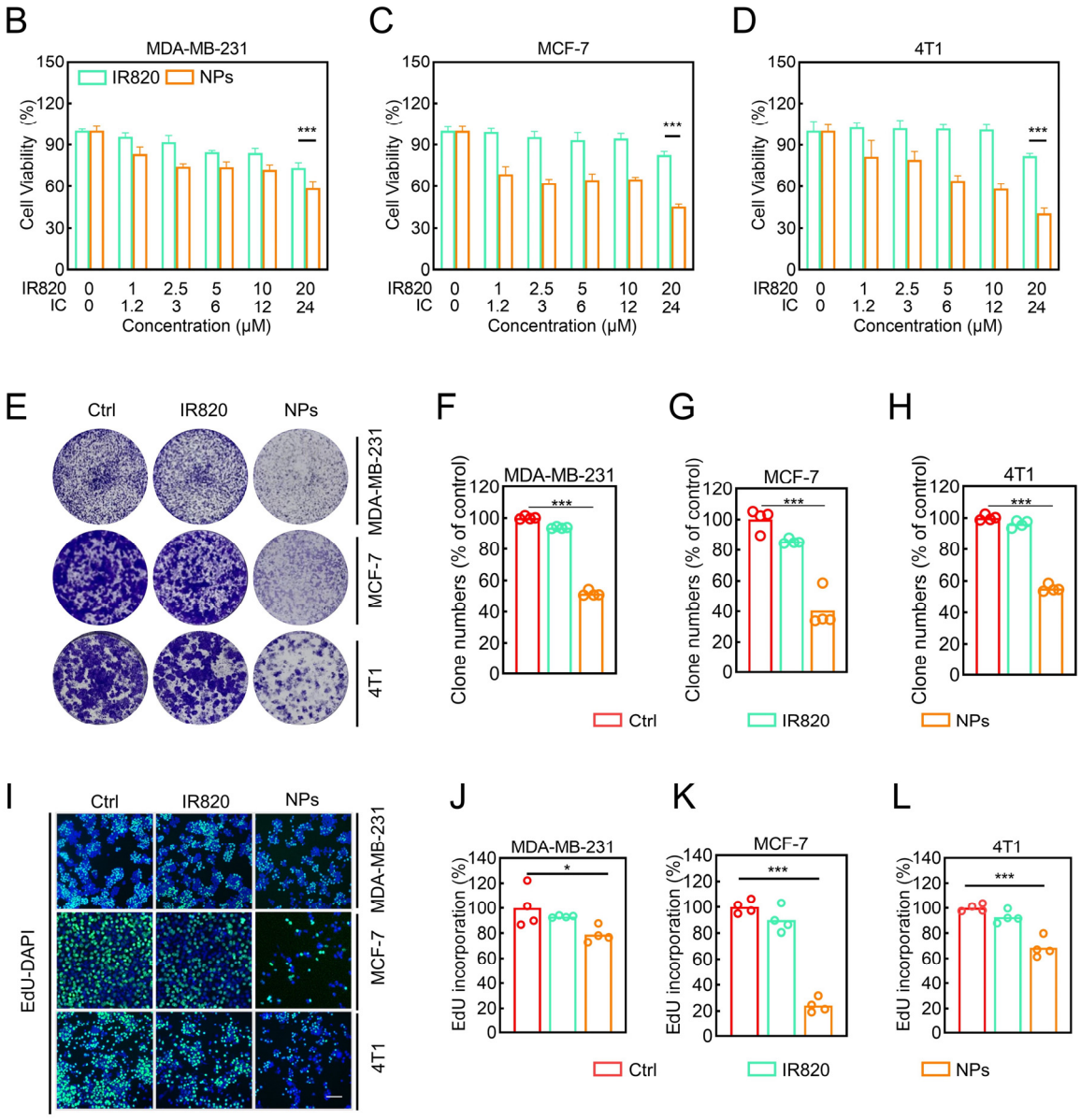

Figure S3. Cytotoxicity of IR820 and IC/IR820 NPs without laser treatment. (A) IC_{50} value of IC/IR820 NPs in different breast cancer cell lines. (B-D) Viability of MDA-MB-231, MCF-

7,4T1 cells co-cultured with IR820, IC/IR820 nanoparticles without laser irradiation. (E-H) Representative images for colony formation of MDA-MB-231, MCF-7,4T1 cells co-cultured with IR820, IC/IR820 nanoparticles without laser irradiation. (I-L) Quantification of the positive ratio of MDA-MB-231, MCF-7, and 4T1 cells co-cultured with IR820, IC/IR820 nanoparticles without laser irradiation in EdU assay. Scale bar: 20 μm.

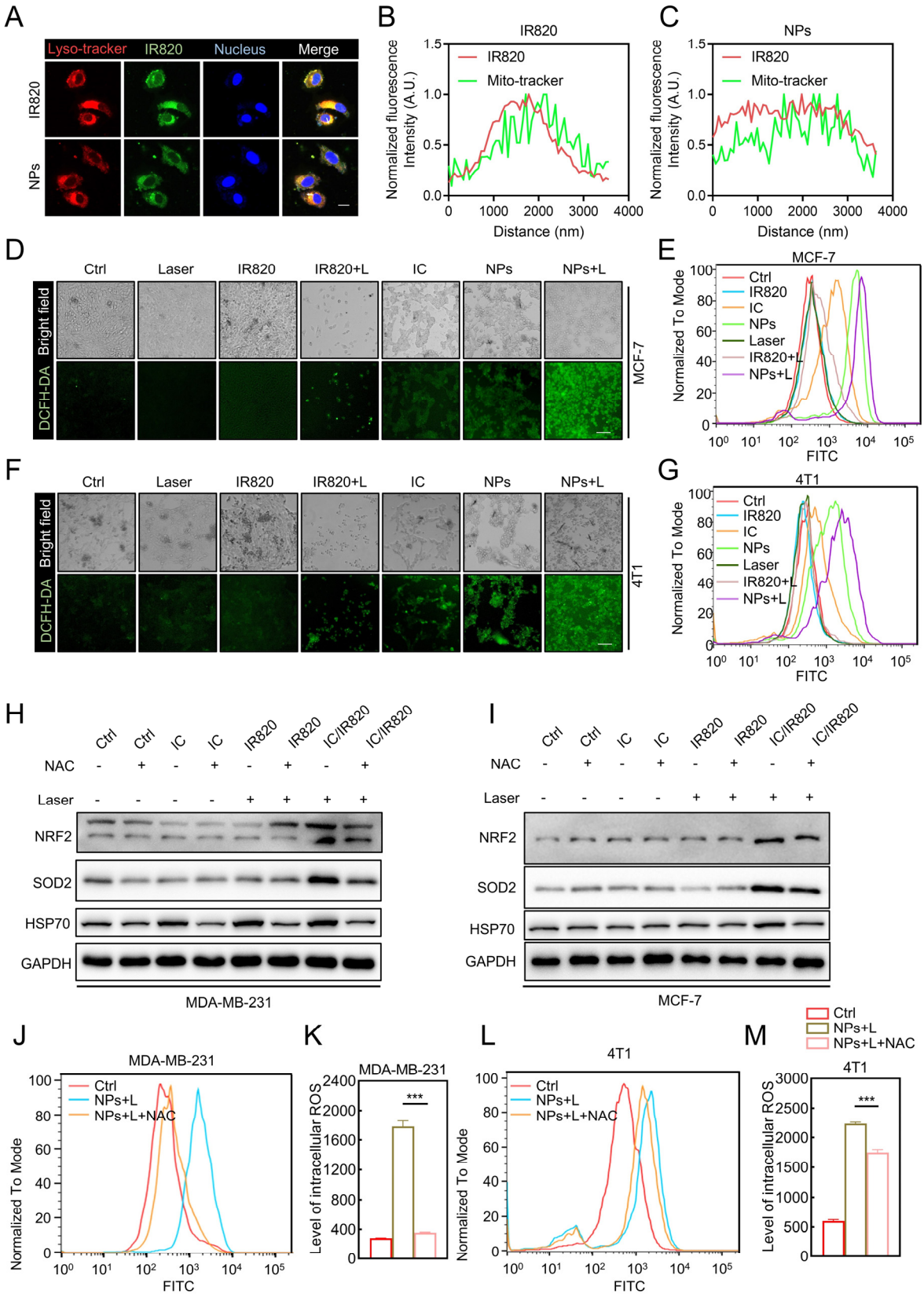
A
Lyso-tracker
IR820
Nucleus
Merge
IR820
NPs
B
IR820
IR820
Mito-tracker
Normalized fluorescence Intensity (A.U.)
Distance (nm)
C
NPs
IR820
Mito-tracker
Normalized fluorescence Intensity (A.U.)
Distance (nm)
D
Ctrl
Laser
IR820
IR820+L
IC
NPs
NPs+L
Bright field
DCFH-DA
MCF-7
E
MCF-7
Ctrl
IR820
IC
NPs
Laser
IR820+L
NPs+L
Normalized To Mode
FITC
F
Ctrl
Laser
IR820
IR820+L
IC
NPs
NPs+L
Bright field
DCFH-DA
4T1
G
4T1
Ctrl
IR820
IC
NPs
Laser
IR820+L
NPs+L
Normalized To Mode
FITC
H
Ctrl
Ctrl
IC
IC
IR820
IR820
IC/IR820
IC/IR820
NAC
Laser
NRF2
SOD2
HSP70
GAPDH
MDA-MB-231
I
Ctrl
Ctrl
IC
IC
IR820
IR820
IC/IR820
IC/IR820
NAC
Laser
NRF2
SOD2
HSP70
GAPDH
MCF-7
J
MDA-MB-231
Ctrl
NPs+L
NPs+L+NAC
Normalized To Mode
FITC
K
MDA-MB-231
Level of intracellular ROS
***
L
4T1
Ctrl
NPs+L
NPs+L+NAC
Normalized To Mode
FITC
M
Ctrl
NPs+L
NPs+L+NAC
4T1
Level of intracellular ROS
***

Figure S4. Cytotoxicity of IC/IR820 NPs is dependent on ROS. (A-C) Immunofluorescence images to show subcellular localization of IR820, IC/IR820 nanoparticles. Scale bar: 20 μm. (D, F) Fluorescence microscopy images and (E, G) flow cytometry analysis for intracellular ROS generation of MCF-7 and 4T1 cells using DCFH-DA as a probe. Scale bar: 20 μm. (λ = 808 nm, P = 1.0 W/cm^2; the irradiation time = 2 min). (H-I) Immunoblot analysis of antioxidant proteins for MDA-MB-231 and MCF-7 cells treated IC, IR820, and IC/IR820 with or without NAC treatment. (λ = 808 nm, P = 1.0 W/cm^2; the irradiation time = 2 min). (J-M) Flow cytometry analysis for intracellular ROS generation of MDA-MB-231 and MCF-7 cells treated IC/IR820 with or without NAC. (λ = 808 nm, P = 1.0 W/cm^2; the irradiation time = 2 min).

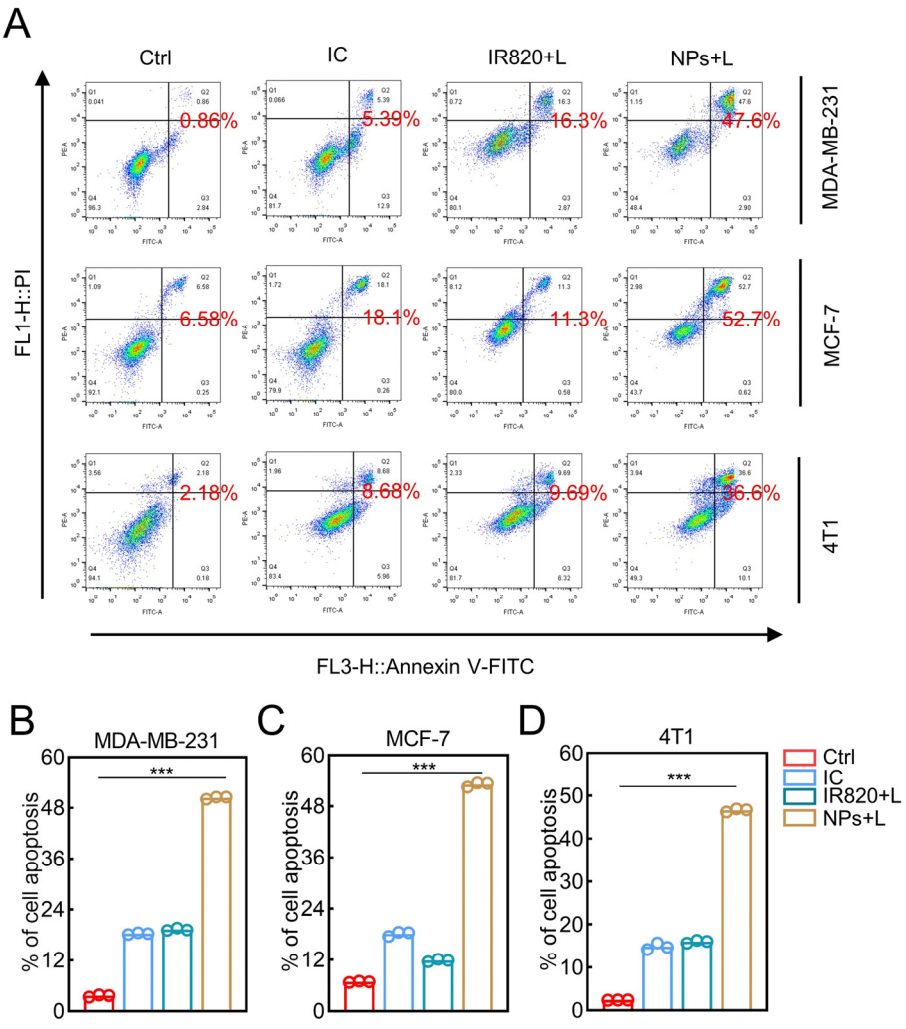

Figure S5. IC/IR820 NPs induce apoptosis in breast cancer cells. (A-D) Apoptosis of IR820, IC, and IC/IR820 NPs were evaluated by annexin V–FITC/PI staining in MDA-MB-231, MCF-7, and 4T1 cells, quantification of apoptotic cell ratio. (λ = 808 nm, P = 1.0 W/cm^2; the irradiation time = 2 min).

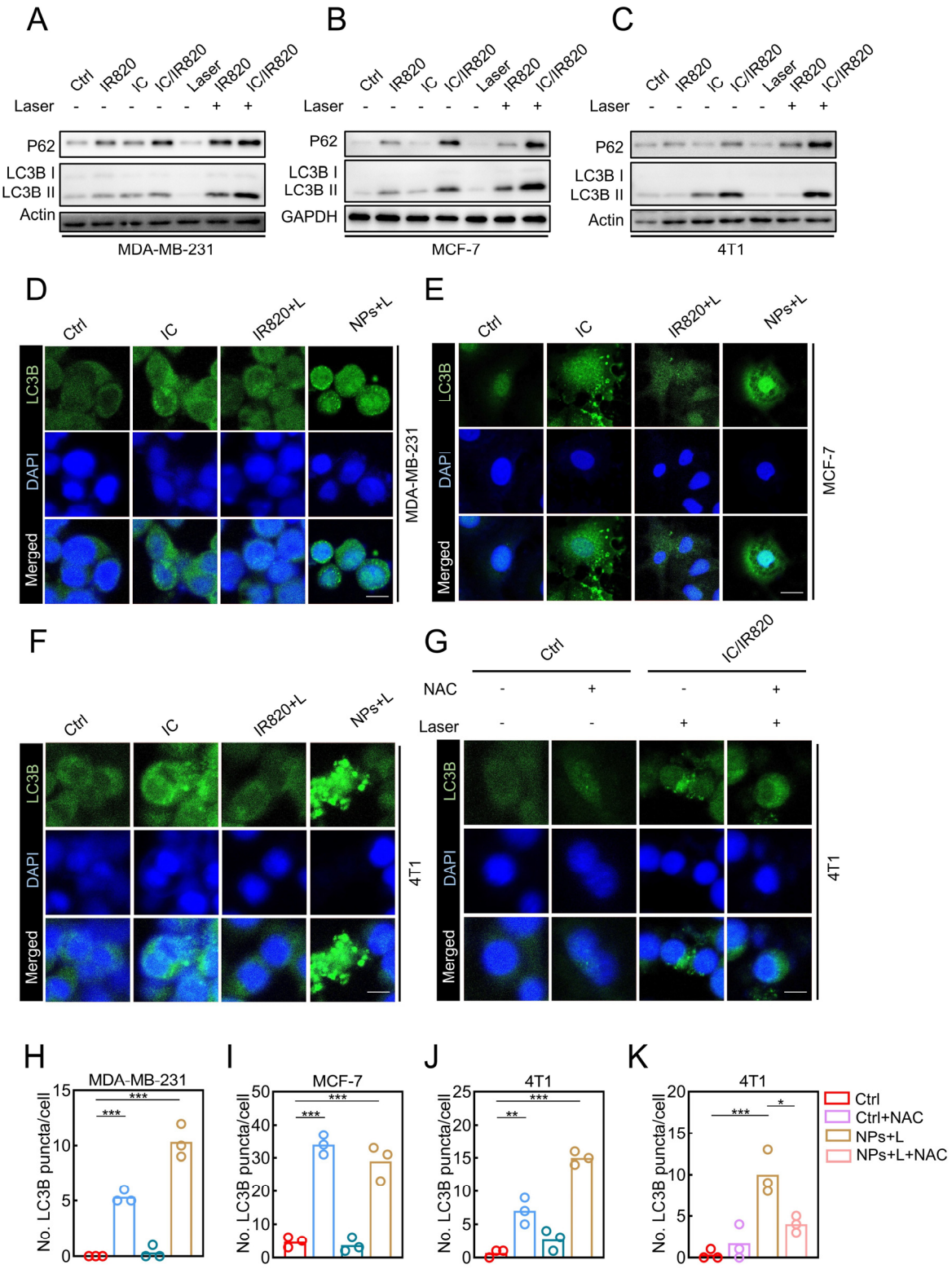
A
B
C
Ctrl
IR820
IC
IC/IR820
Laser
IR820
IC/IR820
Laser - - - - - + +
P62
LC3B I
LC3B II
Actin
GAPDH
MDA-MB-231
MCF-7
4T1
D
E
F
G
Ctrl
IC
IR820+L
NPs+L
LC3B
DAPI
Merged
MDA-MB-231
MCF-7
4T1
NAC - + - +
Laser - - + +
H
I
J
K
No. LC3B puncta/cell
Ctrl
Ctrl+NAC
NPs+L
NPs+L+NAC

Figure S6. IC/IR820 NPs promote autophagy in breast cancer cells. (A-C) Immunoblot analysis of autophagic markers for MDA-MB-231, 4T1, and MCF-7 cells treated IC, IR820, and IC/IR820. (λ = 808 nm, P = 1.0 W/cm^2; the irradiation time = 2 min). (D-F, H-J) Immunofluorescence assays display subcellular localization of LC3B in MDA-MB-231, 4T1, and MCF-7 cells treated IC, IR820, and IC/IR820 NPs, quantification of LC3B puncta per cell. Scale bar: 10 μm. (λ = 808 nm, P = 1.0 W/cm^2; the irradiation time = 30 s). (G, K) Immunofluorescence assays display subcellular localization of LC3B puncta in 4T1 cells treated IC/IR820 NPs with or without NAC treatment, quantification of LC3B puncta per cell. Scale bar: 10 μm. (λ = 808 nm, P = 1.0 W/cm^2; the irradiation time = 30 s).

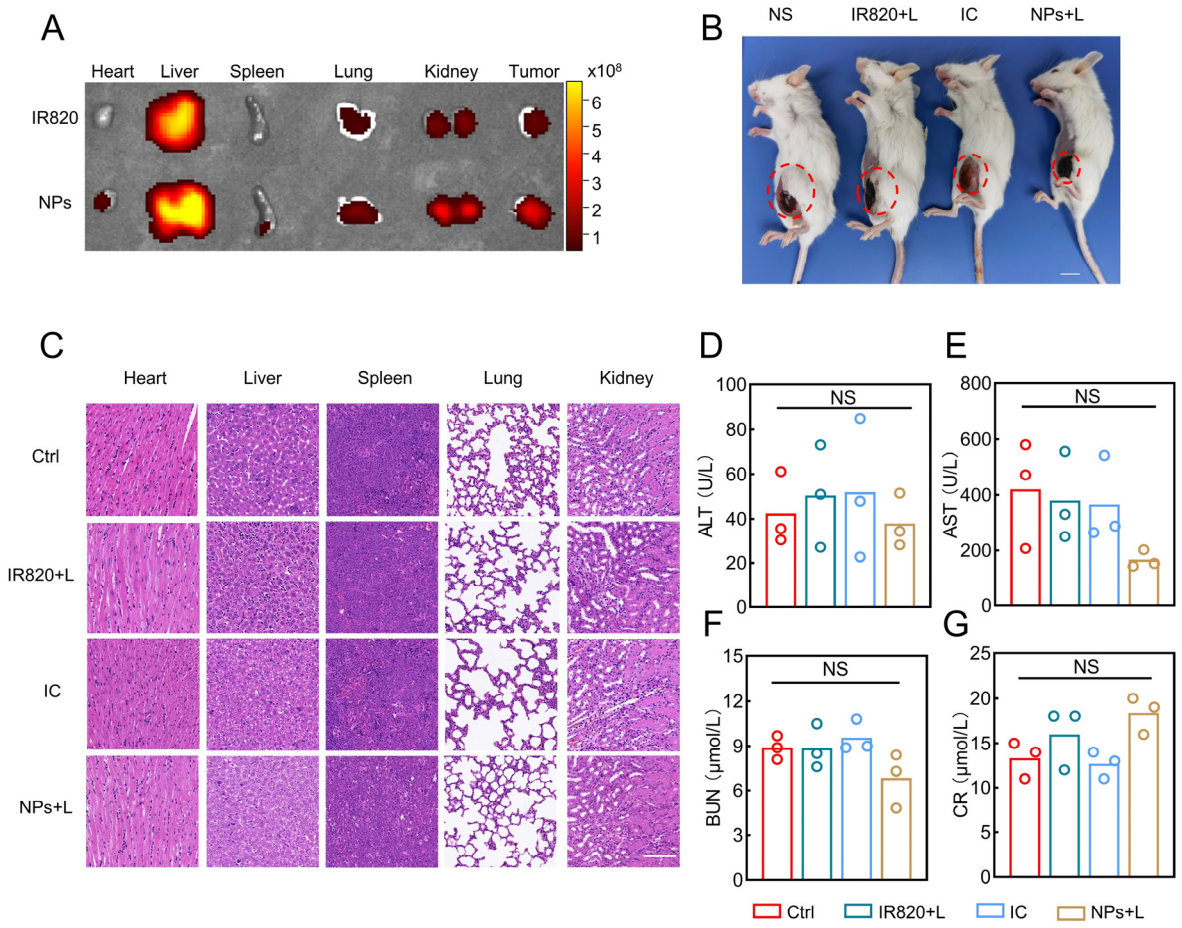

Figure S7. Evaluation of anti-breast cancer effect of IC/IR820 NPs *in vivo*. (A) Fluorescence images of tumors and main organs at 24 h after injection of IR820 and IC/IR820 nanoparticles. (B) Representative images showing tumor size in mice bearing 4T1 orthotopic breast tumor xenografts treated with vehicle, IR820 + Laser, IC, IC/IR820 NPs + Laser at the end of the treatment period. (C) Representative heart, liver, spleen, lung, and kidney HE staining of mice bearing 4T1 orthotopic breast tumor xenografts treated with vehicle, IR820 + Laser, IC, IC/IR820 NPs + Laser at the end of the treatment period. Scar bar: 200 μm. (D-G) Blood biochemical markers: ALT (D); AST (E); BUN (F); CR (G); Each group was tested three times in parallel.

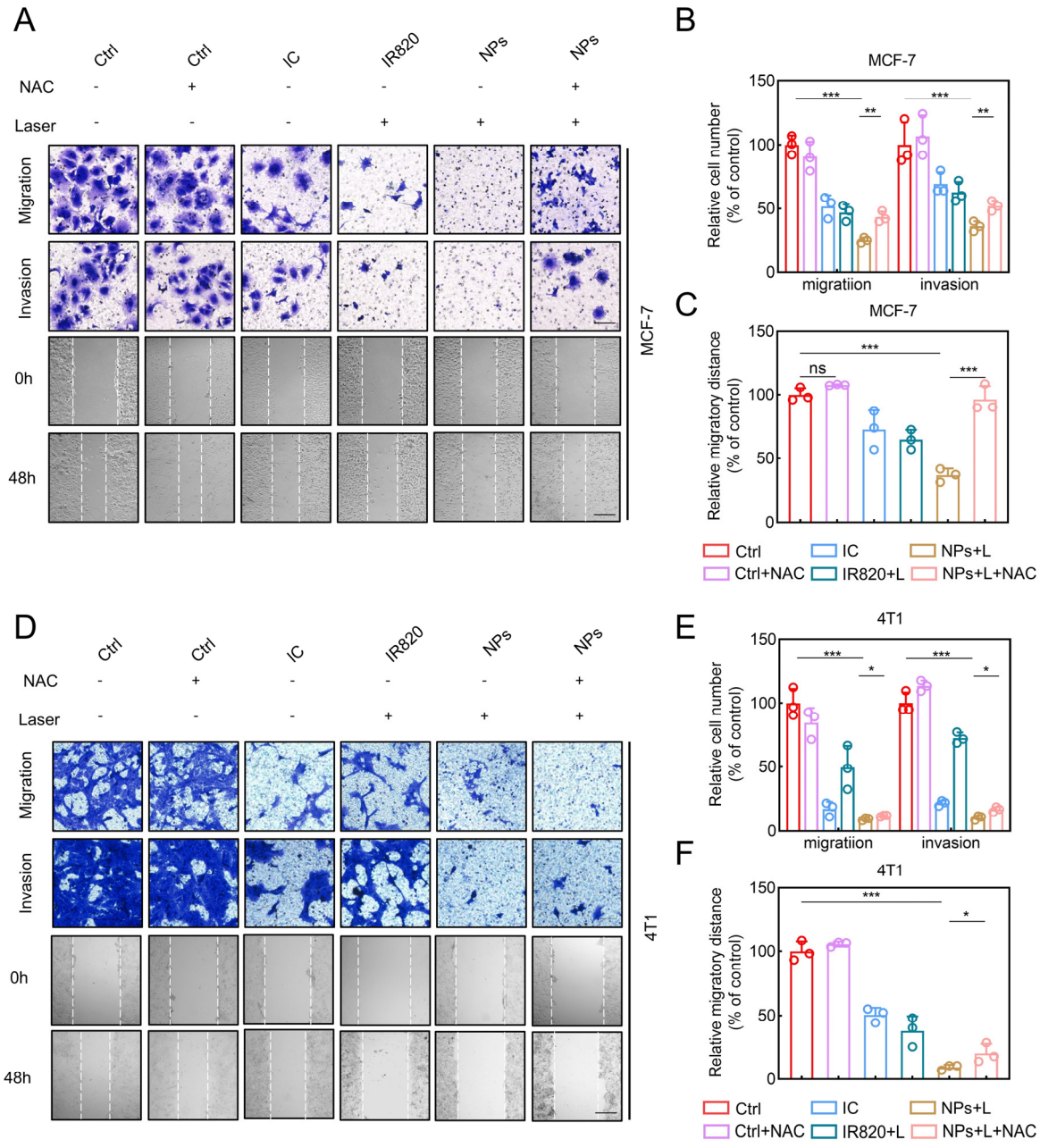

Figure S8. IC/IR820 NPs inhibit migration and invasion of MCF-7 and 4T1 cell line. (A-C) Representative images of migration, invasion, and scratch test of MCF-7 cells, quantification of migration/invasion cell number and migratory distance. Scale bar for migration and invasion assay: 50 μm. Scale bar for scratch test: 20 μm. (D-F) Representative images of migration, invasion, and scratch test of 4T1 cells, quantification of migration/invasion cell number and migratory distance. Scale bar for migration and invasion assay: 50 μm. Scale bar for scratch test: 20 μm.

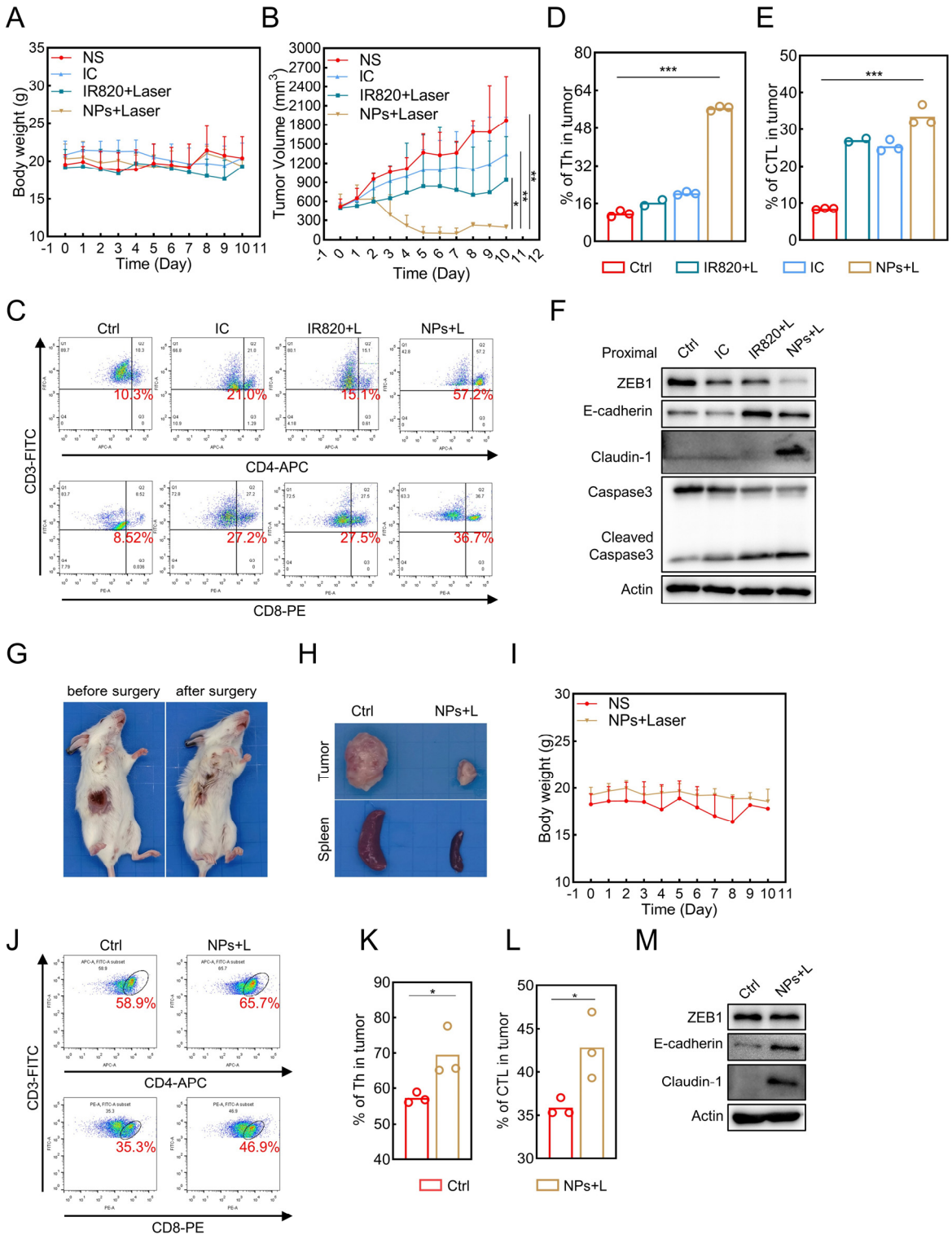
A
Body weight (g)
Time (Day)
NS
IC
IR820+Laser
NPs+Laser
B
Tumor Volume (mm3)
Time (Day)
D
% of Th in tumor
Ctrl
IR820+L
IC
NPs+L
E
% of CTL in tumor
C
Ctrl
IC
IR820+L
NPs+L
CD3-FITC
CD4-APC
CD8-PE
10.3%
21.0%
15.1%
57.2%
8.52%
27.2%
27.5%
36.7%
F
Proximal
ZEB1
E-cadherin
Claudin-1
Caspase3
Cleaved Caspase3
Actin
G
before surgery
after surgery
H
Tumor
Spleen
I
Body weight (g)
Time (Day)
J
58.9%
65.7%
35.3%
46.9%
K
% of Th in tumor
L
% of CTL in tumor
M
ZEB1
E-cadherin
Claudin-1
Actin

Figure S9. IC/IR820 NPs activate the immune response and inhibit breast cancer recurrence. (A) The body weight of mice in each group was measured at the indicated time points. (B) Primary tumor volumes. (C-E) Representative results of $CD4^+$ T cells and $CD8^+$ T cells. Quantification of the percentage of $CD4^+$ T cells and $CD8^+$ T cells in distant tumor. (F) Immunoblot analysis of E-cadherin, caspase3, cleaved-caspase3 for primary tumor treated with NS, IC, IR820, and IC/IR820 NPs. (G-H) Representative images showing tumors and spleens in mice before and after surgery treated with NS or IC/IR820 NPs. (I) The body weight of mice in each group was measured at the indicated time points. (J-L) Representative results of $CD4^+$ T cells and $CD8^+$ T cells. Quantification of the percentage of $CD4^+$ T cells and $CD8^+$ T cells in recurrent tumor. (M) Immunoblot analysis of E-cadherin, claudin 1, HSP70, ZEB1 for recurrent tumor treated with NS or IC/IR820 NPs.